Microsyst Technol (2012) 18:303–309
DOI 10.1007/s00542-012-1431-2

TECHNICAL PAPER

Flip chip solder bump inspection using vibration analysis

Junchao Liu · Tielin Shi · Qi Xia · Guanglan Liao

Received: 16 July 2011 / Accepted: 18 January 2012 / Published online: 2 February 2012
© Springer-Verlag 2012

Abstract Flip chip technology is an attractive choice for high-density packaging and complex microsystem architectures. A critical element in the successful application of flip chip technology is the reliability of solder bumps. In this paper a nondestructive detection method is presented for the flip-chip solder bump inspection using ultrasonic excitation and vibration analysis. Simulations are implemented to explore the feasibility of this method, and experimental investigations are also performed, where the flip chips are excited by continuous ultrasonic waves and their vibration velocities are measured by a laser scanning vibrometer for further analysis. The results reveal that the defective chips can be distinguished from the good chips by the chip vibration velocities with the feature coefficient α, which proves the effectiveness of this method. Therefore, it may provide a new path for the improvement and innovation of flip chip on-line inspection systems.

1 Introduction

As the demands in integration and miniaturization increases, microelectronics fabrication should respond by meeting high-number input/output (I/O) requirements and providing high-density interconnections (Pan et al. 2003). Flip chip technology offers a promising solution with excellent electrical and thermal performance (Elger et al. 2002) owing to the advantages of high I/O counts, short interconnection length (Yoon et al. 2007) and small interconnection resistance (Wolf et al. 2006). During the flip chip packaging process, the mechanical vibration of packaging devices and the thermal expansion mismatch of materials may induce defects to solder bumps, such as missing solder bumps, voids, and cracks (Verma and Han 2004). Since the solder bumps are obscured by the chip and substrate, it is challenging to detect the solder bump defects on flip chips (Tan et al. 2010).

In microelectronics fabrication, current inspection approaches for solder bump inspection include electrical testing, visual inspection, scanning acoustic microscopy (SAM) inspection, and X-ray inspection (Laghari et al. 2011). Electrical testing can detect the defects of a short circuit and open circuit (Wang and Choudhry 2006), but incapable of identifying the intermittent defects such as partial cracks (Martin 1999). Visual inspection is convenient for the quality assessment of wire bonded solder bumps (Yuan et al. 2006). Since the inner solder bumps of flip chips are obscured by the substrate, chip, and external bumps, it is difficult to detect the inner solder bump defects by visual inspection (Kim et al. 1999). In SAM inspection, a coupling medium between the transducer and the specimen is required for impedance matching and coupling the acoustic waves into the specimen (Brand et al. 2010). The coupling media may introduce defects to solder bumps because of the effect of fluid impact. X-ray inspection is a useful tool to isolate and analyze the solder bump defects in a nondestructive way (Chiu and Chen 2006). However, X-ray inspection requires a high degree of operator skill and the equipment is very expensive. Laser ultrasound and thermal imaging technology are also introduced into the

J. Liu · Q. Xia · G. Liao (✉)
State Key Laboratory of Digital Manufacturing
Equipment and Technology, Huazhong University of Science
and Technology, Wuhan 430074, China
e-mail: guanglan.liao@mail.hust.edu.cn

T. Shi
Wuhan National Laboratory for Optoelectronics,
Wuhan 430074, China

solder bump inspection. Yang and Ume (2010) developed a laser ultrasound inspection system to investigate the open solder bumps through modal and signal analysis. Lu et al. (2011) proposed a thermal inspection approach based on the pulsed phase thermography for identification of missing solder bumps.

In this paper a nondestructive inspection method using ultrasonic excitation and vibration analysis is presented for flip-chip solder bump inspection. The test chips with missing solder bumps, a typical defect in flip-chip packaging (Oresjo 2002), are employed as the test samples. A signal generator and a power amplifier are utilized to drive an air-coupled ultrasonic transducer to produce continuous ultrasonic waves for exciting the test chips. The chip vibration velocities are measured by a laser scanning vibrometer and investigated for detecting the missing solder bumps. Then a feature coefficient α is introduced for further analysis. The results of simulation analysis and experimental investigation prove the feasibility of this method.

2 Theoretical basis of ultrasonic excitation and vibration analysis

Ultrasonic excitation is a convenient technique for exciting the small structures in vibration analysis (Heylen et al. 1998). In the ultrasonic field, the transmission of ultrasonic waves causes a transient ultrasonic pressure in the medium (Morse 1948), which can be expressed as $p(\boldsymbol{r},t) = P(\boldsymbol{r})\cos[2\pi ft + \varphi(\boldsymbol{r})]$. Here $\boldsymbol{r}$ is the location vector, t is time, $P(\boldsymbol{r})$ is the amplitude of ultrasonic pressure at $\boldsymbol{r}$, f is the frequency of the ultrasonic waves and $\varphi(\boldsymbol{r})$ is the phase of the ultrasonic waves at $\boldsymbol{r}$. Then an instantaneous energy density $e_f\,(\boldsymbol{r},t) = p(\boldsymbol{r},t)^2/\rho c^2$, derived from the transient acoustic pressure $p(\boldsymbol{r},t)$, will produce an ultrasonic radiation force on the object located in the transmission direction of the ultrasonic waves (Olsen et al. 1958), which can be written as

$$\begin{aligned} F_f(\mathbf{r},t) &= e_f(\mathbf{r},t)d_{\mathbf{r}}(\mathbf{r})dS \\ &= P(\mathbf{r})^2\cos^2[2\pi ft + \varphi(\mathbf{r})]/\rho c^2 \cdot d_{\mathbf{r}}(\mathbf{r})dS. \end{aligned} \quad (1)$$

Here ρ is the medium density, c is the sound speed, $d_{\boldsymbol{r}}(\boldsymbol{r})$ is the drag coefficient (Westervelt 1951), and dS is the area element in the transmission direction of the ultrasonic waves. Huber et al. (2007) utilized the ultrasonic radiation force to excite a MEMS mirror and MEMS gyroscope for modal testing. Kang et al. (2010) exploited the ultrasonic radiation force to excite a micro-cantilever for evaluating its dynamic response. It proved the feasibility of using ultrasonic radiation force to excite the microstructures. Therefore, the ultrasonic waves were applied in this work for exciting the flip chips.

In recent years, vibration analysis has been introduced into the investigation of microstructure. Konofagou and Hynynen (2003) demonstrated that the structures of different stiffness exhibited different displacements under ultrasonic excitation. It indicated that the solder bump defects, inducing the flip-chip stiffness to decrease, could be revealed by the change of vibration parameters. Thus vibration velocities were employed for detecting solder bump defects on flip chips.

3 Experimental setup

The flip-chip test chips obtained from Practical Component were used in this work. The chip dimensions were 5.08 × 5.08 × 0.635 mm. There were 92 eutectic tin–lead solder bumps, 135 μm in diameter with a bump pitch of 254 μm, distributed along the chip edges. To replicate the defects of missing solder bumps, some solder bumps were removed from the chips, as shown schematically in Fig. 1. Then we fabricated the silicon substrates, which were 100 mm in diameter with a thickness of 0.8 mm. The test chips were bonded to the substrates by reflow soldering process.

An experimental system for solder bump inspection was constructed, as displayed in Fig. 2. Continuous sine voltage signals with a frequency of 180 kHz were produced by the signal generator (Polytec, GEN-M2), and magnified by the power amplifier (NJFNKJ, HFVA-62) to enhance the ultrasonic power for better excitation. Through the

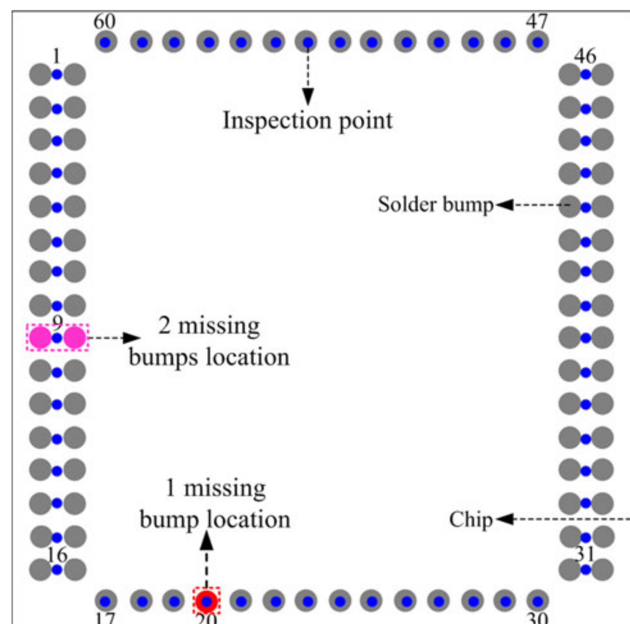

Fig. 1 Schematic diagram of the defect locations with inspection points

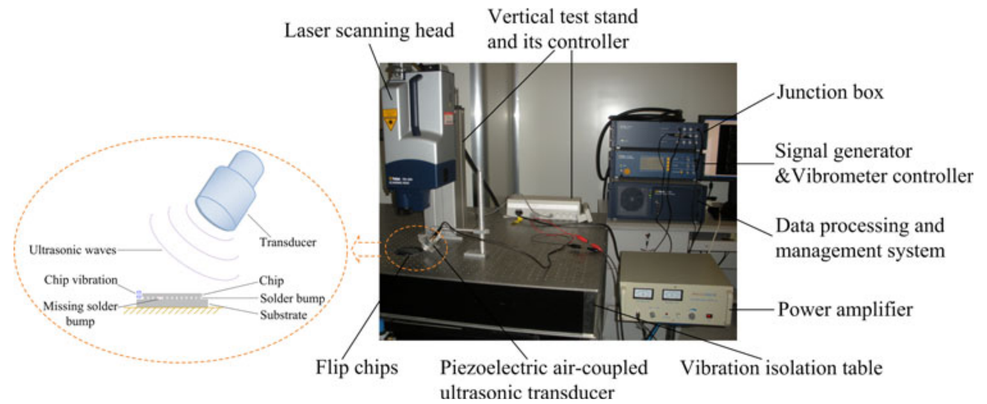

Fig. 2 Experimental system for solder joint inspection

piezoelectric air-coupled ultrasonic transducer (ULTRAN Group, NCG200-D25-P76), these magnified signals were transformed to the ultrasonic waves, which were projected onto the flip chip in continuous-wave mode for exciting the test chips. Compared with the laser pulse excitation (Yang and Ume 2010), the ultrasonic excitation has a narrow bandwidth. It can concentrate the excitation energy in the specific frequency required for testing. The substrate of the test chips was fixed on the vibration isolation table by adhesive tapes. In the experiments, the inspection points were set on the chip surface, as shown in Fig. 1. Their vibration velocities were measured by the laser scanning vibrometer (Polytec, PSV-400) with a sampling frequency of 2.56 MHz. The vibrometer operated on the Doppler principle, measuring the frequency shift of the back-scattered laser light reflected from a vibrating structure to determine its instantaneous velocity. The diameter of the laser spot was 13 μm and the velocity resolution of the vibrometer was 0.02 μm/s.

4 Results and discussion

4.1 Simulation analysis

The finite element simulations were implemented by the application of COMSOL Multiphysics 3.5a software using the acoustic and structural mechanics modules. According to the experimental setup, a physical model was made as shown in Fig. 3a. The acoustic pressure source was set on the inclined plane of the triangular prism as 30 Pa/V in order to imitate the output of the ultrasonic transducer. The triangular prism was 17.678 × 25 × 17.678 mm, representing the air between the flip chip and ultrasonic transducer. The dimensions of the flip chip referred to its actual size. Because of the minor effect on the chip vibration velocity, the under bump metallization layers were omitted (Liu and Ume 2002). The finite element model was shown in Fig. 3b. The solder bumps were manually meshed to improve the mesh uniformity and control the element quantity. However, the chip, substrate, and triangular prism were free-meshed to keep the nodes uniform at the boundary for variable coupling. The finite element model was solved by employing the time dependent solver. In simulation analysis, the inspection points were sited consistent with the experimental setting, and their vibration velocities were obtained from the simulation postprocessing.

Figure 4 displayed the simulation vibration velocities of the chips. The vibration velocities of the defective chips were larger than those of the good chips. For defective chips, the vibration velocities of the chip with two missing bumps were larger than those of the chip with one missing bump, which indicated that the vibration velocities would increase with the addition of missing bumps. Since the vibration period of the chips was 5.56 μs, corresponding to the excitation frequency of 180 kHz which was apart from the chip natural frequency of 200.35 kHz, the influence of natural resonant properties on the velocity variations could be excluded. To investigate the difference on the vibration velocities between the defective chips and good chips, a feature coefficient α was introduced:

$$\alpha = \frac{\frac{\sum_{n=1}^{m}|v_{in}|}{m} - \frac{\sum_{n=1}^{m}|v_{gn}|}{m}}{\frac{\sum_{n=1}^{m}|v_{gn}|}{m}}. \quad (2)$$

Here v_{in} is the velocity amplitude of the inspection point on the defective chip or good chip 2, as schematically shown by the solid circles in Fig. 4; v_{gn} is the velocity amplitude of the corresponding inspection point on the good chip 1; n is the index number of the velocity amplitude, as schematically shown in Fig. 4; m is the total number of the velocity amplitudes, which equals to the maximum index number $n_{\max}$. In this work, $m = n_{\max} = 10$. The α values were calculated according to the velocity amplitudes of the inspection points in Fig. 4 and listed in Table 1. There was an apparent discrepancy in

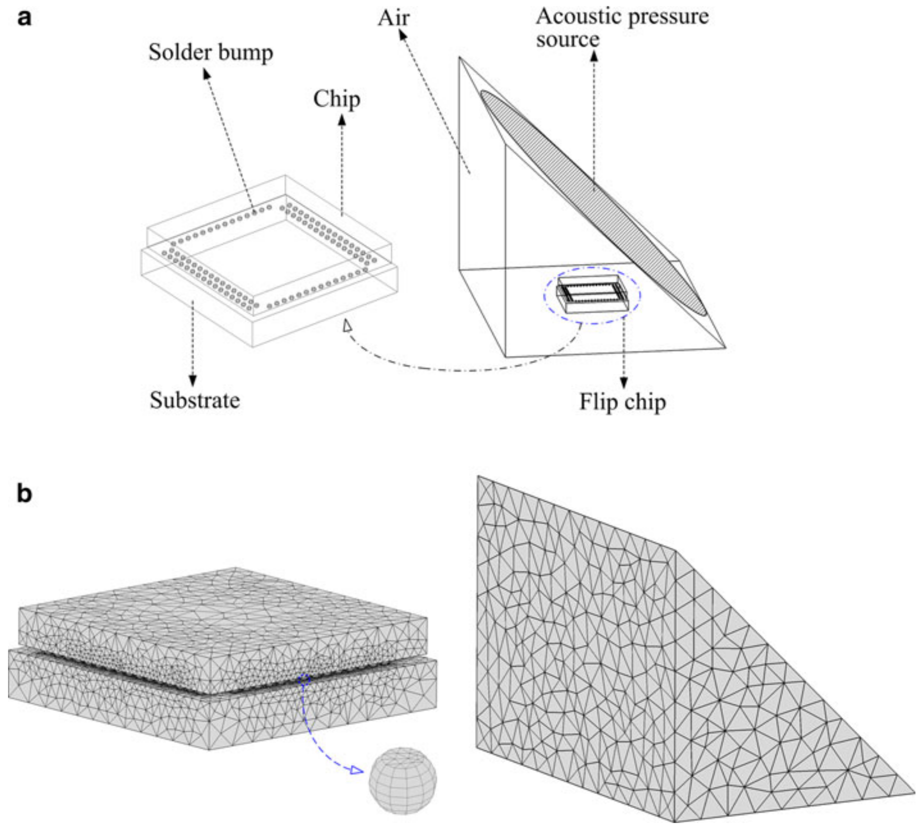

Fig. 3 Simulation model: **a** physical model; **b** finite element model

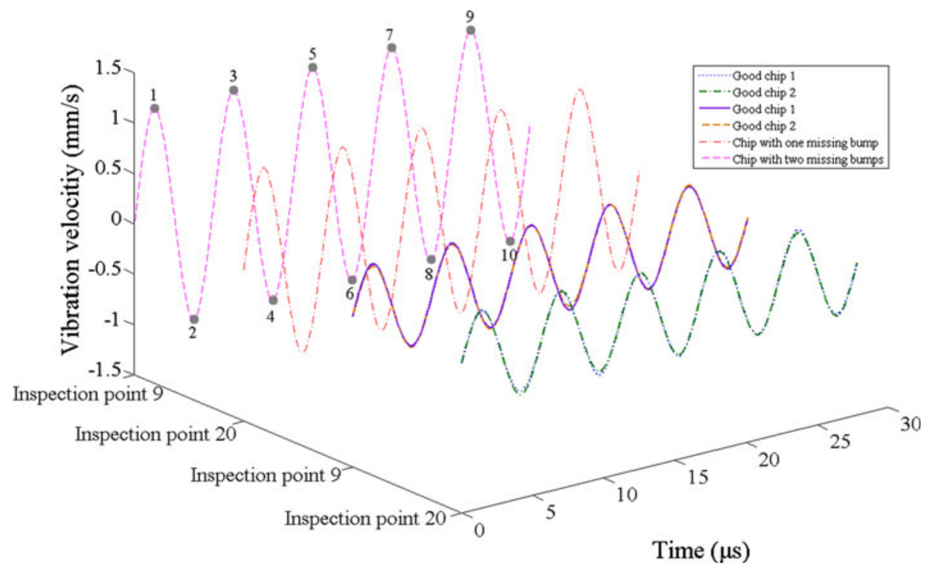

Fig. 4 Simulation vibration velocities of the chips

Table 1 Simulation α values

	Good chip 2		Chip with one missing bump	Chip with two missing bumps
	Inspection point 20	Inspection point 9	Inspection point 20	Inspection 9
Quantity of missing bump	0	0	1	2
α	0.007	0.011	1.089	1.379

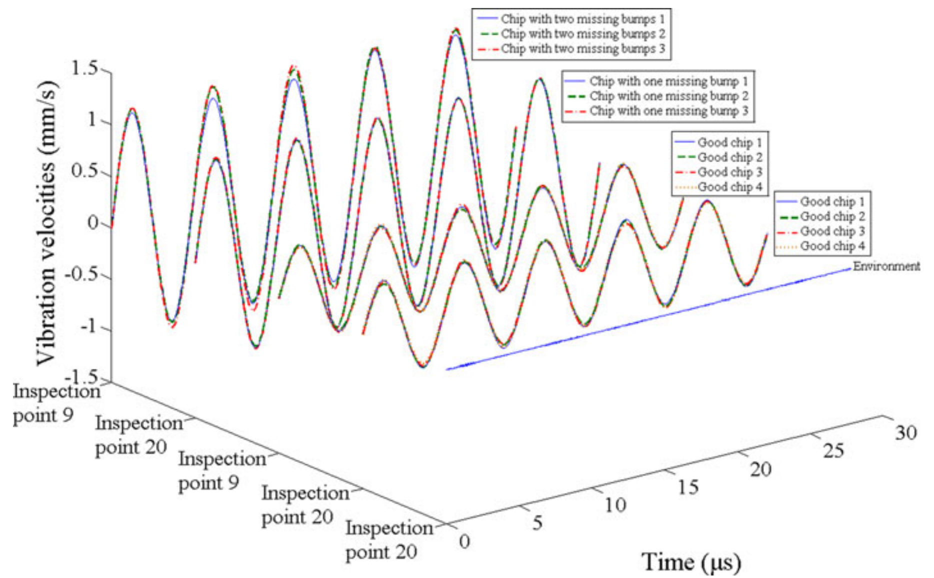

Fig. 5 Experimental vibration velocities of the chips

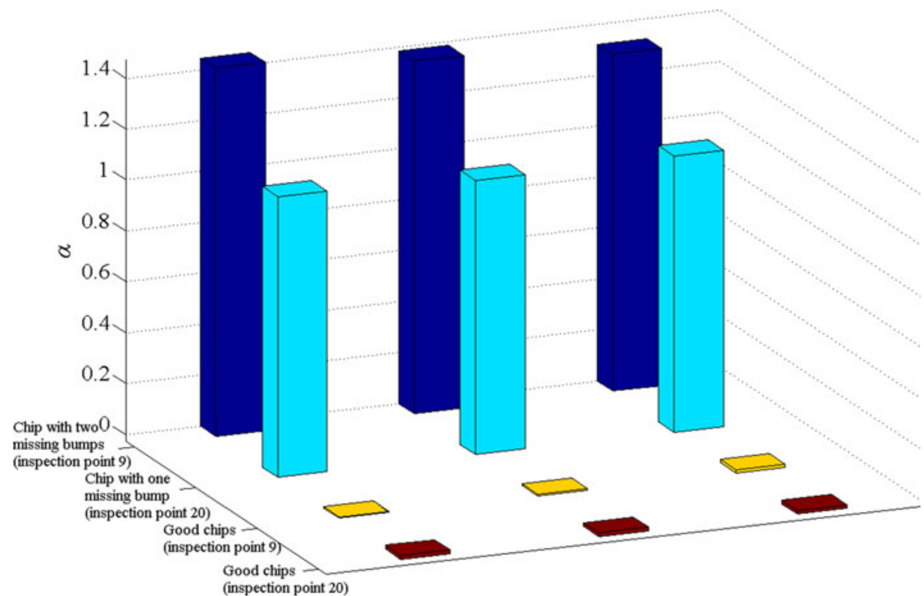

Fig. 6 Experimental α values

α values between the defective chips and good chip, and the α of the defective chips were larger than those of the good chip. It indicated that the defective chips could be distinguished from the good chip by the chip vibration velocities with the feature coefficient α. In addition, the α values increased with the quantity of missing bumps.

4.2 Experimental investigation

Figure 5 depicted the experimental vibration velocities of the chips. The vibration velocities, merely induced by the surrounding environment, were below 0.01 mm/s, which were far less than the vibration velocities under ultrasonic excitation. Thus, the effect of the surrounding environment could be neglected. It also proved the effectiveness of using ultrasonic waves to excite the microelectronic components. Under ultrasonic excitation, the vibration period of the chips was 5.56 μs, corresponding to the excitation frequency of 180 kHz. For the first-order resonant frequency of the chips was 200.35 kHz, apart from the chip vibration frequency, the influence of natural resonant properties on the velocity variations could be excluded. The vibration velocities on the identical inspection point of the good chips are similar, indicating the repeatable coupling of the ultrasonic excitation. For the defective chips, their vibration velocities were larger than those of the good chips, which was consistent with the simulation results. However, there were still some differences on the vibration

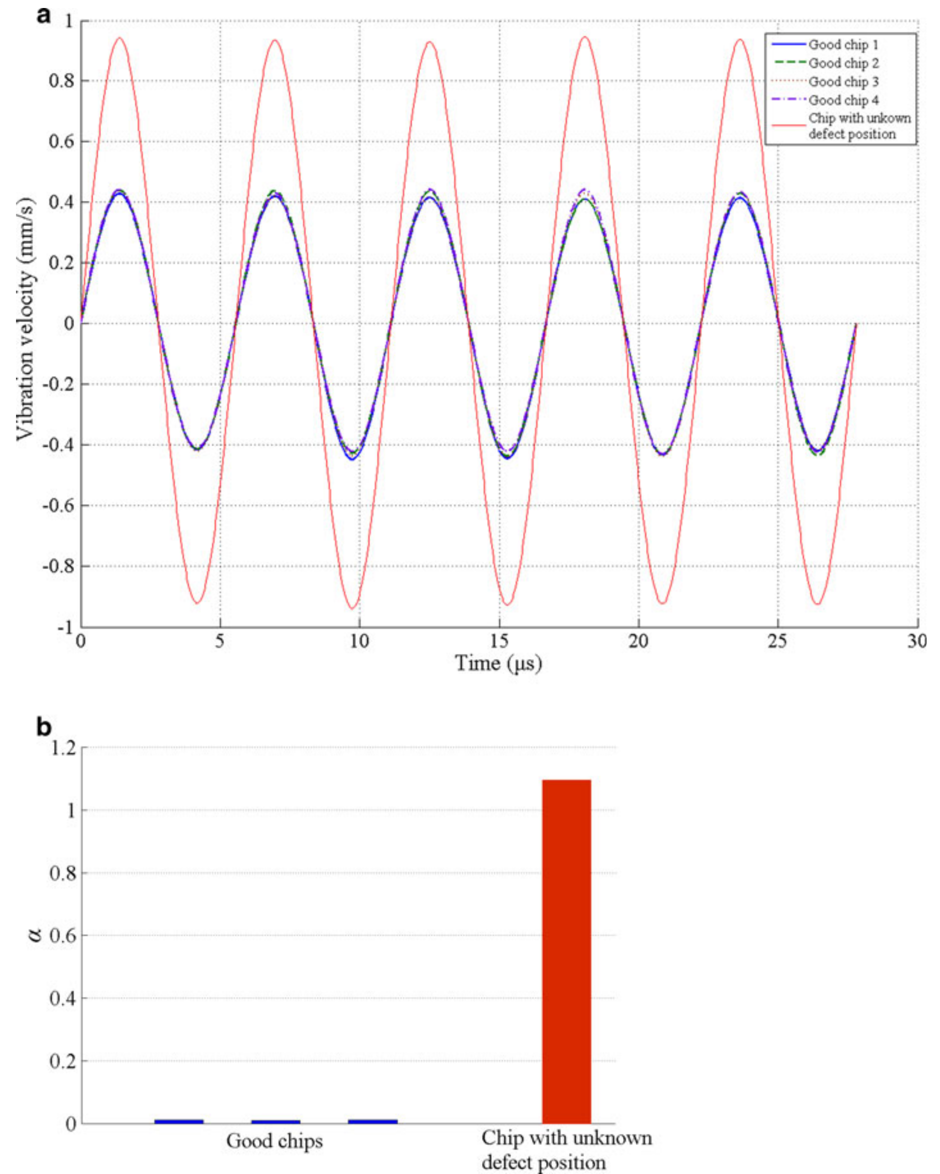

Fig. 7 **a** Vibration velocities of the inspection point 60; **b** α values of the inspection point 60

velocities between the experiments and simulations with a relative error below 2%, because the effects of air damping and flip chip internal damping were difficult to be accurately simulated in the simulations.

Based on the velocity amplitudes of the inspection points in Fig. 5, the experimental feature coefficient α were computed by virtue of Eq. (2). The results were displayed in Fig. 6. The α of the good chips were far less than those of the defective chips, and the α values increased correspondingly with the quantity of missing bumps. This is in accord with the simulation analysis and proved that the defective chips could be distinguished from the good chips by the chip vibration velocities with the feature coefficient α.

To further investigate the feasibility of this method, the chip with unknown defect position was inspected. The distribution of the inspection points was consistent with the experimental setup, and their vibration velocities were measured and shown in Fig. 7a. The vibration velocities of the inspection point 60 on the defective chip were larger than those on the good chips. Then the α of the inspection point were calculated as depicted in Fig. 7b. The α of the

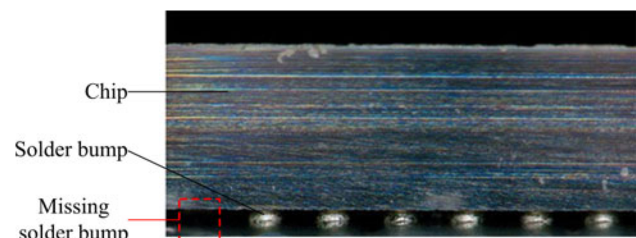

Fig. 8 Solder bumps image of the defective chip

good chips were far less than that of the defective chip. For validation purpose, the solder bumps image of the defective chip derived from the digital microscope (Keyence, VHX-1000) was displayed in Fig. 8. There was one bump missing at the corner, which verified the inspection results of this method.

However, there are some current limitations regarding the practical use of the inspection method. In the actual manufacturing process, the underfiller is applied to fill the gap between the chip and substrate, reducing the thermal stresses on the solder bumps (Moon et al. 2011). The underfiller may reduce the difference on vibration velocities between the defective chip and good chip, but the missing bumps can still be detected through the small difference by employing signal processing techniques. Therefore, the techniques such as wavelet analysis will be introduced to improve this inspection method in the next work. In addition, more complicated defects such as open solder bumps, fatigue cracks, and their combinations will also be introduced and investigated for extending the application scope of this method.

5 Conclusion

This paper proposed a nondestructive inspection method combining ultrasonic excitation with vibration analysis for flip-chip solder bump inspection. Simulations were implemented to explore the feasibility of this method. In the experiments, the flip chips with artificial defects were excited by ultrasonic waves in continuous-wave mode, and their vibration velocities were measured by the laser scanning vibrometer and further analyzed. The results of simulation analysis and experimental investigation prove that the defective chips can be distinguished from the good chips by the chip vibration velocities with the feature coefficient α. Hence this method may provide a new path for the improvement and innovation of flip chip on-line inspection systems.

Acknowledgments This work was supported partially by the National Fundamental Research Program of China (Grant No. 2009CB724204) and National Natural Science Foundation of China (Grant No. 50975106).

References

Brand S, Czurratis P, Hoffrogge P, Petzold M (2010) Automated inspection and classification of flip-chip-contacts using scanning acoustic microscopy. Microelectron Reliab 50:1469–1473

Chiu SH, Chen C (2006) Investigation of void nucleation and propagation during electromigration of flip-chip solder joints using X-ray microscopy. Appl Phys Lett 89(26):1–3

Elger G, Hutter M, Oppermann H, Aschenbrenner R, Reichl H, Jager E (2002) Development of an assembly process and reliability investigations for flip-chip LEDs using the AuSn soldering. Microsyst Technol 7(5–6):239–243

Heylen W, Lammens S, Sas P (1998) Modal analysis theory and testing. Katholieke Universitiet Leuven, Belgium

Huber TM, Fatemi M et al. (2007) Noncontact modal excitation of small structures using ultrasound radiation force. In: Proceedings of the SEM annual conference and exposition on experimental and applied mechanics 1 pp 604–610

Kang X, He XY, Tay CJ, Quan C (2010) Non-contact evaluation of the resonant frequency of a microstructure using ultrasonic wave. Acta Mechanica Solida Sinica 26:317–323

Kim TH, Cho TH, Moon YS, Park SH (1999) Visual inspection system for the classification of solder joints. Pattern Recogn 32(4):565–575

Konofagou EE, Hynynen K (2003) Localized harmonic motion imaging theory simulations and experiments. Ultrasound Med Biol 29(10):1405–1413

Laghari MS, Hijer R, Khuwaja GA (2011) Efficient techniques for BGA solder joint identification in low resolution X-ray images. IEEE GCC Conf Exhib 2011:128–131

Liu S, Ume C (2002) Vibration analysis based modeling and defect recognition for flip-chip solder-joint inspection. J Elect Packaging 124(3):221–226

Lu XN, Liao GL, Zha ZY, Xia Q, Shi TL (2011) A novel approach for flip chip solder joint inspection based on pulsed phase thermography. NDT E Int 44(6):484–489

Martin PL (1999) Electronic failure analysis handbook. McGraw-Hill, New York

Moon SW, Li ZH, Gokhale S, Wang JL (2011) 3-D numerical simulation and validation of underfill flow of flip-chips. IEEE Trans Compon Packaging Manuf Technol 1(10):1517–1522

Morse PM (1948) Vibration and sound. McGraw-Hill, New York

Olsen H, Wergeland H, Westervelt PJ (1958) Acoustic radiation force. J Acoust Soc Am 30(7):633–634

Oresjo S (2002) New study reveals component defect levels. Circuits Assembly 39–43

Pan LW, Yuen P, Lin L, Garcia EJ (2003) Flip chip electrical interconnection by selective electroplating and bonding. Microsyst Technol 10(1):7–10

Tan YC, Tan CM, Ng TC (2010) Addressing the challenges in solder resistance measurement for electromigration test. Microelectron Reliab 50:1352–1354

Verma K, Han B (2004) Real-time observation of thermally induced warpage of flip-chip package using far-infrared Fizeau interferometry. Exp Mech 44(6):628–633

Wang ZF, Choudhry M (2006) A study of flip-chip open solder bump failure mechanism. In: ISTFA 2006—32nd international symposium for testing and failure analysis 2006, pp 239–242

Westervelt PJ (1951) Theory of steady force caused by sound waves. J Acoust Soc Am 23(4):312–315

Wolf MJ, Engelmann G, Dietrich L, Reichl H (2006) Flip chip bumping technology—status and update. Nucl Instrum Methods Phys Res A 565:290–295

Yang J, Ume C (2010) Laser ultrasonic technique for evaluating solder bump defects in flip chip packages using modal and signal analysis methods. IEEE Trans Ultrason Ferroelectr Freq Control 57(4):920–932

Yoon JW, Chun HS, Koo JM, Jung SB (2007) Au–Sn flip-chip solder bump for microelectronic and optoelectronic applications. Microsyst Technol 13(11–12):1463–1469

Yuan S, Tian DP, Zeng YX (2006) 3D inspection on wafer solder bumps using binary grating projection in integrated circuit manufacturing. IEICE Trans Electron E89-C(5):602–606